Diamond & Related Materials 160 (2025) 112994

Contents lists available at ScienceDirect

Diamond & Related Materials

journal homepage: www.elsevier.com/locate/diamond

Dynamic effects of incomplete ionization in edge terminations of diamond power devices☆

Martin Kah *, Nazareno Donato, Florin Udrea

Cambridge University, Department of Engineering, Electrical Engineering Division, Cambridge, UK

ARTICLE INFO

Keywords:
Diamond
Incomplete ionization
Diamond devices
Technology Computer-Aided Design (TCAD)

ABSTRACT

The transient response of junction termination extensions (JTEs) in diamond-based Schottky diodes is critically influenced by the incomplete ionization of dopants under high electric fields and fast-switching conditions. Using an extended TCAD simulation framework that includes time-dependent ionization kinetics, we demonstrate that the limited ionization speed of phosphorus donors under fast voltage ramps leads to transient JTE charge reduction. This, in turn, degrades field management at the device edge and triggers premature avalanche breakdown, significantly reducing the effectiveness of conventional JTE structures. To address this limitation, we propose a hybrid edge termination approach that integrates phosphorus-doped JTEs with oxide field plates. This design maintains high termination efficiency under slow switching conditions while substantially restoring field control during fast transients, improving robustness across a wide operational range. Our findings underline the importance of accounting for dynamic ionization effects in the design of ideal edge terminations for diamond-based power devices, similar to observations in other wide-bandgap semiconductors.

1. Introduction

State-of-the-art diamond devices, either diodes or transistors, have evolved into high-performance prototypes [1,2], driven by the up-scaling of substrate availability and improvements in crystal quality [3,4], along with the refinement of fabrication processes [5] associated with this promising material for high-power, high-temperature, and harsh-environment applications. Advances in device design and modelization have been initiated and supported by theoretical predictions, often relying on the substitution of diamond material parameters into physical models originally developed for silicon [6,7], which may have caused over-prediction or in general incorrect predictions of diamond device performances. Despite the efficiency of simulation routines for early-stage device concepts, the use of models and design approaches originally developed for silicon reaches its limits and may need to be revisited for diamond. Termination design is still an issue, fabrication-wise but also simulation-wise where, accurate modelling of all relevant physical mechanisms is crucial for understanding the impact of diamond's specific properties on device behaviour and for enabling effective design and optimization strategies.

One of the central limitations in diamond electronics is the deep ionization levels of available dopants, such as substitutional boron acceptors (0.38 eV above the valence band maximum) and substitutional phosphorus donors (0.58 eV below the conduction band minimum), which result in incomplete ionization at room temperature (RT). While this effect is negligible in silicon, except for very low temperatures, it is well established that in ultra-wide bandgap semiconductors, incomplete ionization significantly limits carrier availability in bulk-conduction devices, ultimately increasing the series resistance [8]. Although this limiting factor for static on-state conduction has been well documented and experimentally demonstrated in p-type diamond Schottky barrier diodes (SBDs) [9–11], its influence on transient device behaviour, particularly under fast-switching conditions, has so far only been theoretically explored for diamond [12]. In contrast, such effects have already been reported in 4H- and 6H-SiC pn-diodes subjected to single-shot reverse bias pulses, where a reduction in the statically measured breakdown voltage was observed [13]. Further studies on 4H-SiC transistors and super-junctions, have shown that the delayed generation of free carriers from non-ionized dopants and deep traps in the high-field region of the depletion zone contributes to the dynamic lowering of the breakdown voltage [14,15]. In diamond, due to its even higher dopant activation energies, these transient effects are expected to be more pronounced, potentially limiting device robustness if not properly mitigated.

☆ This article is part of a Special issue entitled: 'NDNC2025' published in Diamond & Related Materials.

* Corresponding author.
E-mail address: mryk2@cam.ac.uk (M. Kah).

https://doi.org/10.1016/j.diamond.2025.112994
Received 6 August 2025; Received in revised form 13 October 2025; Accepted 20 October 2025
Available online 22 October 2025

To investigate this, we extend conventional drift–diffusion simulations by incorporating balance equations for dopant ionization, using theoretically estimated time constants. Using TCAD simulations, we refine the modelling of avalanche-induced breakdown in Schottky barrier diodes (SBDs) under single-shot reverse bias pulses. This approach enables a more accurate evaluation of transient electric field distributions and carrier dynamics in SBDs, thereby supporting improved optimization of edge termination regions. Although previous simulations have demonstrated junction termination efficiencies exceeding 90% [16–18], key limiting factors, such as dynamic dopant ionization, have so far been neglected. The aim of this work is to refine TCAD simulations of SBD edge terminations by explicitly incorporating dynamic ionization effects, with the goal of proposing optimized diode edge termination strategies. A detailed understanding of the interplay between ionization kinetics, temperature, and device architecture is crucial for advancing ideal edge termination design in diamond and for realizing the full potential of this material in high-performance power electronics.

2. Theory

Modelling of the incomplete ionization in diamond is often done by conceiving the dopant species as acceptors and donors impurities coupled with the valence and conductance bands, respectively, within the framework of the electrothermal drift–diffusion model [19]. Providing that hydrogenoid model is valid, deep-level impurities are regarded with the Fermi–Dirac distribution, also known as the steady-state Gibbs distribution [20], and the ratio of ionized donors at thermal equilibrium follows the subsequent equations:

$$\frac{N_D^+}{N_{D0}} = \frac{1}{1 + g_D \exp\left(\frac{E_{Fn} - E_D}{k_B T}\right)} \tag{1}$$

where E_{Fn} is the quasi-Fermi energy level for electrons, N_D^+ is the ionized donor density, affiliated to the donor density N_{D0}, the degeneracy factor g_D for donors, and the thermal energy is expressed as the product of the Boltzmann constant k_B and the temperature T. The resulting ionization ratio is plotted in Fig. 1(a) and (b) for Nitrogen and Phosphorous, respectively, at various temperatures. The ionization energies of the principal n-type dopants, nitrogen and phosphorus, as well as the primary p-type dopant, boron, are indicated in the inset of Fig. 1(a).

The very high activation energy of nitrogen results in a negligible fraction of ionized donors at room temperature (RT), explaining the insulating behaviour of nitrogen-doped diamond under these conditions, in contrast to phosphorus-doped diamond. These ionization fractions further decrease at lower temperatures as the quasi-Fermi level in n-type semiconductors shifts closer to the conduction band edge. A similar expression can be derived for acceptors using the same steady-state Gibbs distribution framework, as already applied in the modelling of p-type diamond and 4H–SiC [14,15]. While some wide and ultra-wide bandgap semiconductors exhibit both shallow and deep dopants, oxygen-terminated diamond, particularly in devices that rely on bulk conduction as focused on in this paper, suffers from deep levels for both dopant species. It is worth noting that for n-type diamond, the Pearson–Bardeen model, which accounts for a reduction in activation energy at high doping concentrations, has not been included here due to the lack of reproducible experimental validation in diamond, despite the existence of empirical models [21]. Similarly, ionization energy modifications due to the Poole–Frenkel [22] effect have been neglected in this work.

While Eq. (1) is valid under electro-thermal equilibrium and in bulk regions, the dynamic ionization rate necessitate the use of a new set of equations which regulate dopant activation. The later is described through the generalization of the Shockley–Read–Hall model in the particular case of transient condition, hence it is highly dependent on the electrons, capture c_n, and emission e_n, rates [23]. Evolution of the ionization fraction as function of time is expressed as:

$$\begin{aligned} \frac{\partial\left(\frac{N_D^+}{N_{D0}}\right)}{\partial t} &= -\frac{1}{\tau_n} \times \frac{N_D^+}{N_{D0}} + e_n \\ \tau_n &= \frac{1}{e_n + n \times c_n} \\ c_n &= \upsilon_e^{th} \times \sigma_n \\ e_n &= \upsilon_e^{th} \times \sigma_n \times \frac{N_C}{g_D} \times \exp\left(-\frac{E_C - E_D}{k_B T}\right) \end{aligned} \tag{2}$$

where N_C is the density of state in the conduction band, υ_e^{th} is the mean electron thermal velocity, n the free electron charge density and σ_D the dopant capture cross section. The ionization time constant τ_n characterizes the charge/discharge relaxation time of electrons associated with a donor level at energy $E_C - E_D$. A similar formulation can be applied for acceptor impurities. Typically, if the variation in free electron concentration occurs on a timescale shorter than τ_n, the ionization or neutralization of donors cannot follow the external excitation instantaneously. In such cases, the quasi-static approximation, which assumes an effectively instantaneous response due to a negligible ionization time constant, is no longer justified.

The change in ionized doping concentration and of its time derivative resulting from (2) are computed with Poisson's equation and the electron continuity equation, respectively. Particular case holds when derivation is made within a space charge region (SCR), as in the vicinity of a pn-junction interface, where no free carriers are available in the structure, hence $\tau_n = 1/e_n$. Under this specific condition, the time constant does not depend upon the capture rate and it can be easily evaluated as shown in Fig. 1(c) for Nitrogen-doped, and (d) Phosphorous-doped diamond. It is worth noting that, for nitrogen, variations in the capture cross-section have a low practical impact on the ionization time constant, as the associated time scales already exceed several billion years at room temperature. In contrast, for phosphorus-doped diamond, τ_n range from a few milliseconds to several tenths of a second, introducing potential reliability concerns for fast-switching device applications. The effects of fast reverse bias pulses on the modelling of a pn-junction, used within a SBD junction termination extension (JTE) will be discussed in the next section.

3. Results and discussions

3.1. Models and design

To mitigate and reduce the electric field crowding at the device periphery and avoid premature breakdown, various termination techniques, such as field plates (FP) [18], field guard rings (FGR) [24], or junction termination extensions (JTE) [16], have been proposed but only FPs and FGRs have been successfully implemented in diamond devices [25]. However, the full potential of these methods has been difficult to realize experimentally due to fabrication challenges and material quality limitations, preventing them from matching the high termination efficiencies predicted by simulations. A key drawback of field plate termination is the elevated electric field seen by the oxide, often triggering premature failure before avalanche. Especially, time dependent dielectric breakdown (TDDB) and hot carrier injection constitute critical reliability concerns arising from the high electric field stress imposed on the dielectric layer. The JTE, by contrast, relieves this pressure from the oxide and redistributes the peak field into the semiconductor itself, where it can be more safely sustained. However, even if JTEs is expected to be more resilient than FPs, questions remain as to whether all relevant parameters have been adequately taken into account in these studies, and whether developing n-type diamond might be necessary to fully exploit the benefits of this approach.

The cross-sectional view of the unit cell for the pseudo-vertical diamond Schottky barrier diode (SBD) with phosphorus-doped junction

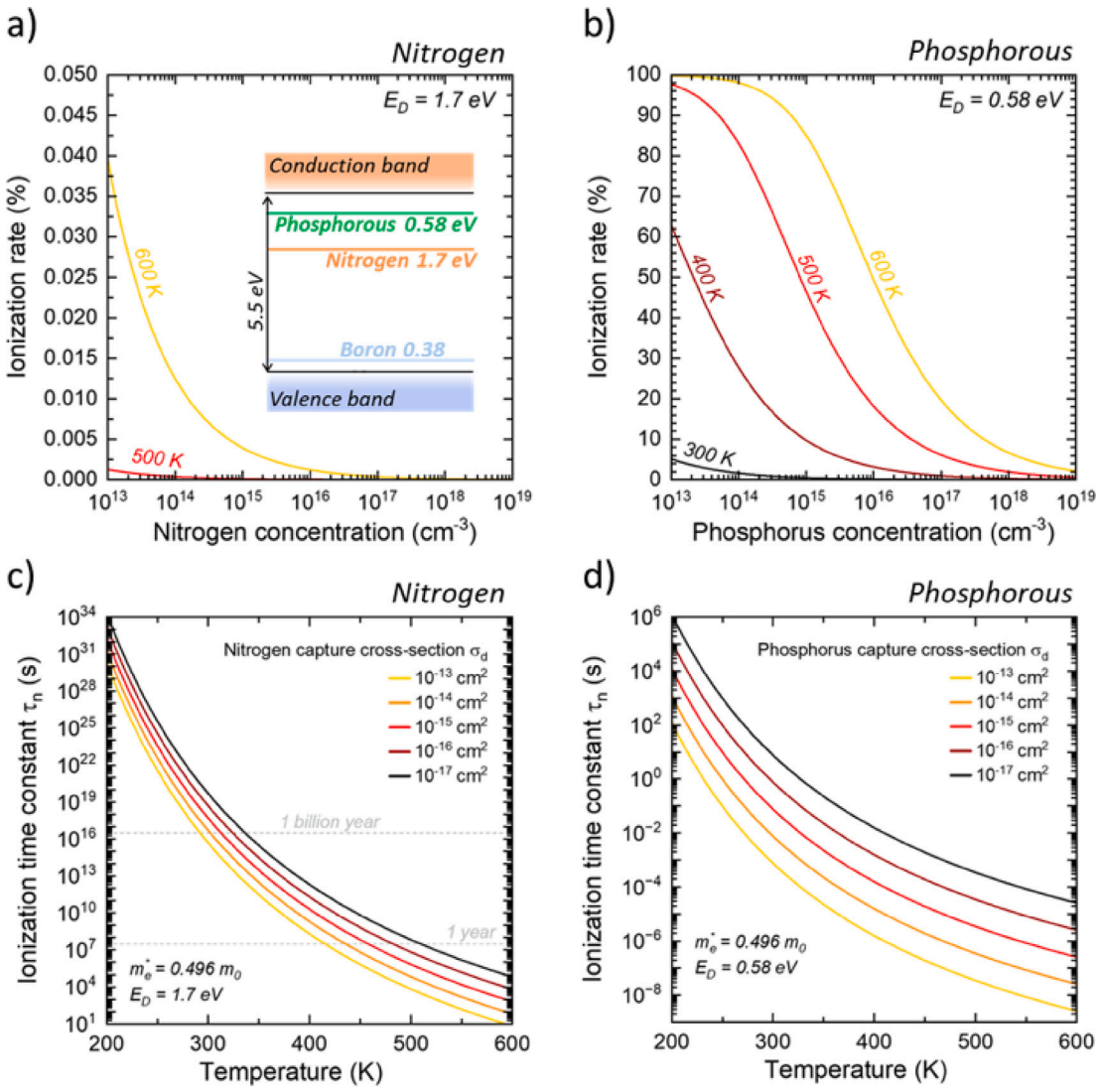

Fig. 1. (a) Ionization rate as function of Nitrogen concentration at 500–600 K, and (b) for Phosphorous with temperature ranging between 300 and 600 K. Inset in figure (a) represents the energy levels of common dopants in diamond relative to the conduction and valence bands. (c) Ionization time constant (τ_n) of Nitrogen, and (d) for Phosphorous as a function of temperature for various capture cross-sections, ranging between 10^{-17} and 10^{-13} cm^2.

termination extension (JTE) is presented in Fig. 2(a), highlighting all relevant structural parameters. In terms of fabrication, the structure can be implemented through n-type implantation followed by deep etching, although both techniques remain challenging for diamond. Alternatively, a more robust approach may involve shallow etching followed by in situ n-doped epitaxy and planarization with a subsequent deep etch. On the simulations, a central point is the implementation of incomplete ionization: for the p-type layer, ionization energy varies with doping concentration [26], while for the n-type region, a constant ionization energy is assumed. These effects are incorporated into the TCAD models along with temperature- and doping-dependent carrier mobility [27,28]. To provide a detailed analysis, focus is made upon n-type diamond integrated inside SBD edge termination, but the results presented alongside this section are valid for any pn-junction based devices, fabricated with ultra-wide bandgap semiconductors that suffer from incomplete ionization.

The diode breakdown is modelled as an avalanche process, using an impact ionization model with coefficients established by Hiraiwa et al. and incorporating temperature dependence [29]. Specifically, a positive temperature dependence of the ionization coefficients has been incorporated to account for the interaction between accelerated carriers (electrons and holes) and the phonon gas [30,31]. However, simulation presented in this work are not electro-thermal and this effect will be studied in a separate publication. Under these assumptions, for a p-layer thickness of 6.5, μm and a doping concentration of 10^{16} cm^{-3}, the estimated ideal 1D breakdown voltage is approximately 2.8 kV, placing the device in the punch-through regime [32]. The Schottky barrier height is fixed at 1.3 and while leakage mechanisms may contribute to premature avalanche, here we focus exclusively on breakdown driven by impact ionization. We assess blocking performance using several methods, for example, by detecting a sudden rise in current due to impact ionization and by calculating the corresponding ionization integral.

The capture cross sections for nitrogen and phosphorus dopants are set to 10^{-17} cm^2 unless otherwise specified. This conservative lower-bound value emphasizes critical cases, although experimental studies report disparate values for Phosphorous ranging between 10^{-15} cm^2 and 10^{-19} cm^2 [33,34], while limited results on Nitrogen reported value around 10^{-15} cm^2 [35]. In the simulations presented here, the cross section is kept independent of temperature and electric field to highlight its role in this study; however, in reality, this parameter may reasonably vary with both temperature and electric field. Nevertheless, due to ongoing challenges in doping control and measurement accuracy, capture cross sections for carriers in diamond impurities, as well

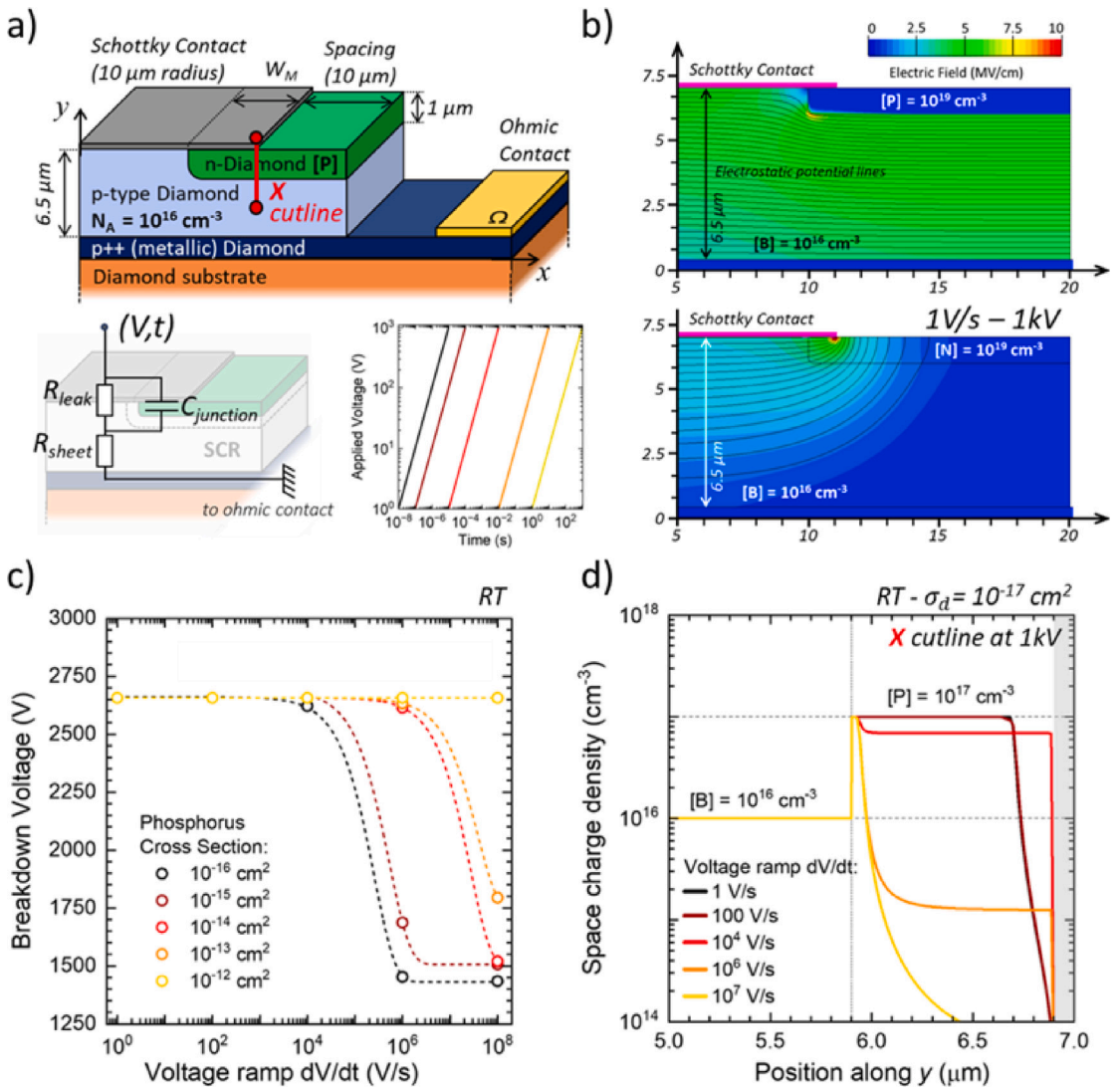

Fig. 2. (a) Schematic cross-section of the simulated diamond-based SBD structure with all the relevant structural parameters. Below, simplified equivalent small-signal schematic of the driving circuit alongside the reverse voltage ramps applied on the Schottky contact. (b) 2D electrostatic simulations at room temperature (RT) and 1 kV bias, illustrating electric field and potential line distributions for phosphorus- (top) and nitrogen-doped (bottom) JTEs. Results obtained through the use of Nitrogen doped diamond are similar to an un-terminated SBD. (c) Simulated breakdown voltage as a function of voltage ramp rate (dV/dt) for different phosphorus capture cross-sections (σ_n). Faster ramps and smaller σ_n values yield lower breakdown voltages due to insufficient ionization. (d) Simulated space charge profiles along the cutline shown in (a) at 1 kV for different ramp rates. Incomplete ionization under fast transients causes significant depletion of space charge near the surface.

as temperature dependence of impact ionization coefficients remain significant and uncertain parameters.

Electric field profiles and electrostatic potential lines for the SBD structure, employing either phosphorus- or nitrogen-doped JTE, are shown in Fig. 2(b). The junction is assumed to be highly asymmetric, with an n-type doping concentration of 10^{19}cm^{-3}, to maximize theoretically the electrostatic extension of the SCR. The field profiles are extracted at a reverse bias of 1 kV, following a linear voltage ramp with a rate of 1 V/s, corresponding to a total ramp duration of 1000s. Highlight of the driving circuit as well as voltage ramps applied are depicted in Fig. 2(a).

It is evident that when using deep substitutional nitrogen donors, the JTE is ineffective in mitigating the peak electric field crowding at the edge of the Schottky contact. In this case, the field distribution is essentially indistinguishable from that of a structure without any JTE. This is further confirmed by the peak electric field beneath the Schottky contact edge, which exceeds 10 MV/cm, significantly higher than the critical electric field in undoped diamond. Conversely, with phosphorus-doped JTE, the peak electric field is efficiently displaced from the Schottky contact edge and redistributed towards the edge of the formed pn-junction, where it is substantially mitigated. This behaviour aligns with the expectations based on the vastly different ionization dynamics: due to the extremely high ionization time constant of nitrogen in diamond, on the order of billions of years at room temperature (see Fig. 1(c)), the electrostatic equilibrium cannot be reached on practical time scales. For this reason, only phosphorus-doped JTE structures are considered in the subsequent analysis. Nonetheless, all simulations presented in this work could, in principle, be extended to nitrogen-doped structures by applying an appropriate time scale.

However, Phosphorous-doped JTE can also be treated as efficient up to an extend of 2 kV/s as demonstrated in Fig. 2(c). Below this value, the displacement of the SCR imposed by the reverse bias rise, is aligned with the rate of change, each steps can be treated and solved through electrostatic integration of Gauss–Poisson's equation. This pivotal value corresponds precisely to the point where the transient switching speed drops below τ_n at room temperature, as illustrated in Fig. 1(d). However, for faster dV/dt, this proportionality is not respected any more,

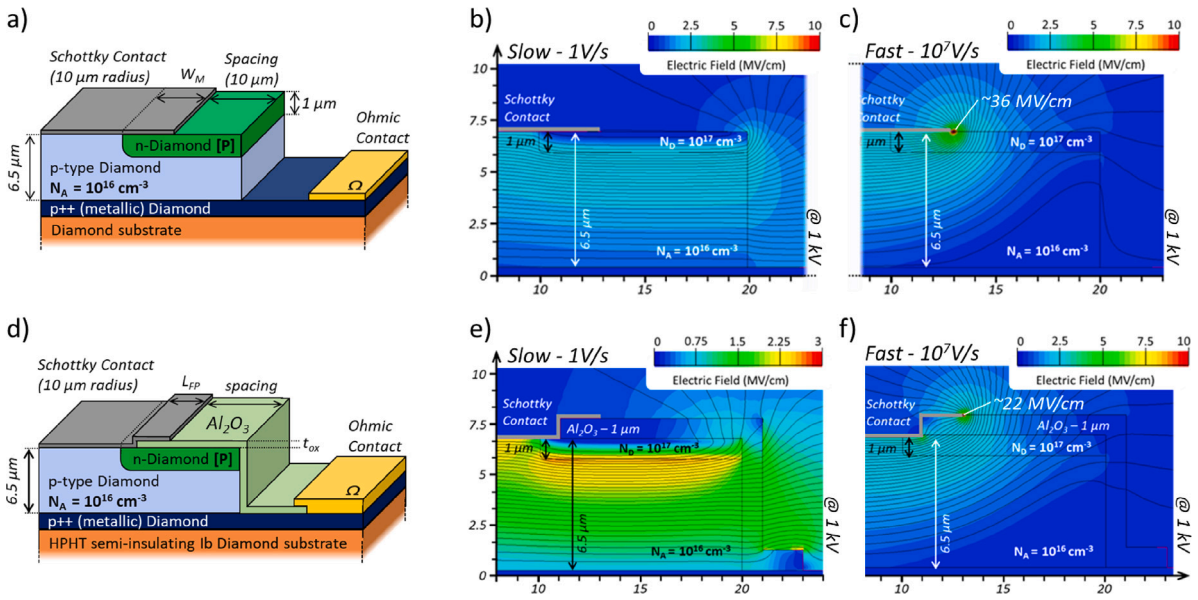

Fig. 3. (a–c) Device structure and electrostatic field distribution for a conventional phosphorus-doped JTE, with: (a) Schematic cross-section of the simulated, diamond-based SBD with JTE-only. (b) Simulated electric field distribution at 1 kV under a slow voltage ramp (1 V/s), showing effective field spreading and termination, and (c) under a fast ramp (10^7 V/s), incomplete dopant ionization leads to severe field crowding and premature breakdown near the Schottky contact. (d–f) Proposed hybrid edge termination integrating oxide field plate with: (d) schematic cross-section of the modified structure, featuring a 1 μm thick Al_2O_3 field plate, with a length of 3 μm. (e) At 1 kV and 1 V/s, the hybrid design further enhances field spreading and suppression of peaks electric field at the edge of the device mesa's. (f) Under fast transients (10^7 V/s), the peak electric field is transferred inside the oxide layer, as the JTE was absent.

and the breakdown voltage (BV) estimated through the impact ionization integral going way above the unity in mixed mode simulations [29], is cut in half compared to previous case. The JTE efficiency, defined as the ratio of the computed BV and the ideal 1D BV, is then lowered to 50%, as for an unterminated SBD. Charge unbalance is illustrated in Fig. 2(d), in which the simulated space charge density in each sides of the pn-diode is plotted at several time steps, or voltage ramp, at a fixed voltage (1 kV) and at RT. As the voltage ramp is faster, only the small fraction of donors ionized at thermal equilibrium (less than 1%, as shown in Fig. 1(b)) contributes to the space charge needed to sustain the applied bias. Consequently, a gradual ionization of non-ionized Phosphorous donors occurs in an expanding region around the pn-junction. Due to the absence of free electrons in this depletion region, this process is limited by the characteristic time constant τ_n. Once the time $t > \tau_n$ has elapsed and the maximum bias has been reached and assuming the voltage is held constant thereafter, the width of the depletion region converges towards the quasi-static case, comparable to the result obtained for a dV/dt of 1 V/s. During this delay, electrons emitted from still unionized donors into the high-field region of the depletion layer contribute to the impact ionization integral, increasing the onset of avalanche breakdown.

3.2. Towards ideal device termination

Although quasi-static simulations suggest that Phosphorous-doped JTE structures is able to maintain the peak electric field inside diamond layers, compared to oxide encapsulation with Field Plate (FP) architectures [18,36], this paper demonstrates that under dynamic conditions (voltage dV/dt, or current dI/dt), the effectiveness of JTE is significantly reduced due to the incomplete ionization of deep n-type dopants. As shown in the electric field profiles in Fig. 3(b) and (c), under fast-switching conditions, the JTE becomes effectively inactive, resulting in field distribution identical to those of a device without any termination. However, architectural modifications can still enhance the breakdown robustness under quasi-stationary or slow ramp conditions. Fig. 3(b) illustrates the electric field mitigation within the effective operating range of a JTE-terminated SBD. The results reveal that the peak electric field is displaced along the vertical n-type diamond mesa edge due to the crowding of equipotential lines at the mesa's corner. This localized field enhancement can lead to premature breakdown, particularly in the presence of fabrication imperfections [37]. To address this, we propose a hybrid edge termination strategy that combines the advantages of the JTE termination with oxide encapsulation and the field plate architecture (Fig. 3(d)). The field plate termination is expected to be less susceptible to fast dV/dt effects due to the lower sensitivity of the majority dopant species (boron) to dynamic ionization effects, which are more severe for phosphorus and nitrogen based JTE terminations. Therefore, the hybrid termination concept can rely on a dual working principle: the JTE determines the field distribution under slow transients and static conditions, while the field plate becomes dominant during faster voltage transitions. This co-contribution ensures a flat efficiency window across all dV/dt and, at the same time, minimizes electrical stress on the passivation.

Aluminium oxide (Al_2O_3) is among the most widely used dielectrics for diamond power devices, particularly on oxygen-terminated surfaces, due to its excellent interface quality, chemical stability, and favourable electronic properties [38,39]. The band alignment at the Al_2O_3/O-diamond interface, as characterized by Maréchal et al. [40], has been used within the calculations presented in this paper. This study also further supports Al_2O_3 suitability for O-terminated diamond encapsulation by ensuring a strong barrier to charge injection, either for electrons and holes.

At low voltage ramp rates (dV/dt), the presence of encapsulation oxide along the vertical sidewalls of the diamond mesa structure allows for significant mitigation of the peak electric field. As shown in Fig. 3(e), the electric field linearly decreased across the oxide thickness, reducing the field crowding at the Schottky contact edge and helping to delay the onset of premature breakdown. This field-spreading effect is particularly effective when the junction termination extension (JTE) is active and fully ionized, allowing the oxide to complement the action of the n-doped termination. This combined configuration of JTE and field-plate oxide achieves a termination efficiency as high as 99.5% for $dV/dt < 100$ V/s, as summarized in Fig. 4.

Under fast-switching conditions, the electric field profiles (Fig. 3(c)) reveal a pronounced crowding beneath the Schottky contact edge,

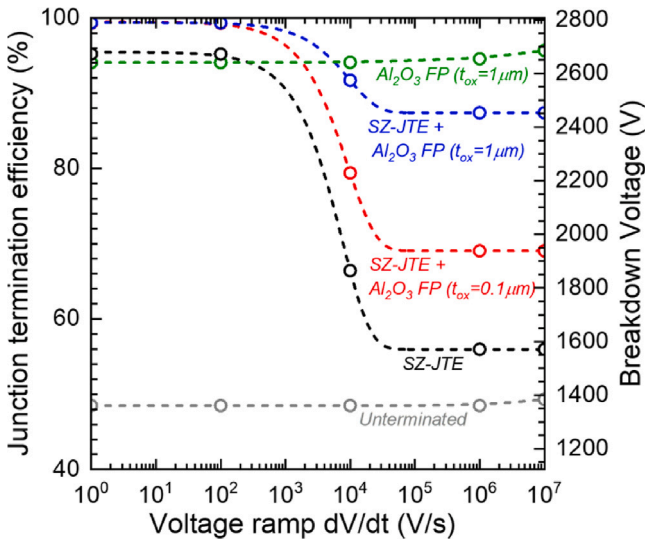

Fig. 4. Junction termination efficiency (Simulated BV/Ideal 1D BV) and simulated BV as function of voltage ramp rate (dV/dt) for different device architecture. SZ-JTE refers to single-zone JTE.

similar to what is observed in the absence of any JTE. However, in such conditions, the added FP architecture begins to play a dominant role. When the JTE effectiveness collapses under high-speed transients, the FP structure provides a backup mechanism by extending the equipotential lines and redistributing the electric field across the oxide layer. This complementary action helps mitigate the reduction in breakdown voltage observed under fast-switching, thus maintaining partial protection and ensuring more robust device operation. In this analysis, oxide breakdown is not considered, so caution is required when interpreting peak electric field values within the oxide. Albeit, because the field plate is predominantly stressed only under fast transients, the hybrid concept is expected to have minimal impact on long-term oxide reliability. However, since breakdown is assumed to occur via avalanche in the diamond itself, the oxide must be thick enough to withstand elevated surface fields in any cases.

To ensure high termination efficiency across both slow and fast dV/dt regimes, a sufficiently thick oxide is essential, as effective field mitigation and surface passivation under fast-switching conditions strongly depend on oxide thickness [41], as illustrated in Fig. 4. Even better prospects are expected using high-k dielectrics, such as Si_3N_4 [1] or ZrO_2 [42]. It is important to emphasize that while dynamic effects are shown here to hinder the performance of JTE-terminated diamond SBD, the very same phenomena underpin the innovative concept of non-volatile photo-switching, using nitrogen-doped diamond [43,44], offering access to near-permanent memory as supported by the analysis presented in this work.

4. Conclusion

This study demonstrates that dynamic dopant ionization plays a critical role in determining the breakdown behaviour of diamond Schottky barrier diodes, specifically when n-doped junction termination extensions are employed. By extending conventional TCAD simulations to incorporate time-dependent dopant ionization kinetics, we show that the transient response of n-type dopants, particularly phosphorus, can substantially degrade the effectiveness of JTEs under fast-switching conditions. When the rate of voltage increase exceeds the ionization capability of phosphorus donors, above 1 kV/s, the resulting charge imbalance leads to a premature onset of avalanche breakdown, resulting in a reduction in termination efficiency, dropping to below 60%. In order to mitigate this limitation, we propose and evaluate a hybrid edge termination strategy that combines phosphorus-doped JTEs with field-plate architectures using oxide encapsulation. This design offers the highest termination efficiency, above 99.5%, under slow voltage ramp conditions, providing complementary field control, and restores significant termination efficiency under fast transient, significantly improving breakdown robustness over a wider switching operation range. For fast switching conditions exceeding 100 kV/s, a 100 nm-thick oxide layer combined with a field-plate architecture increases the termination efficiency to 69%, whereas, in the absence of the oxide, the efficiency of a single-zone JTE termination is limited to 56%. Our results highlight the necessity of considering dynamic ionization effects in the design of edge terminations for diamond-based devices, and the importance of integrating both electrostatic and transient effects into simulation frameworks. As lab-grown single crystal diamond quality never stop to increase, future work should aim to refine dopant capture cross-section measurements and impact ionization models for diamond. The later will helps to design resilient charge compensation techniques to improve the dynamic response of various diamond-based devices design. Ultimately, the insights presented here provide a foundation for the reliable design of diamond power devices capable of operating under increasingly stringent switching requirements.

CRediT authorship contribution statement

Martin Kah: Writing – review & editing, Writing – original draft, Methodology, Investigation, Formal analysis, Data curation. **Nazareno Donato:** Writing – review & editing, Visualization, Validation, Methodology, Investigation, Conceptualization. **Florin Udrea:** Writing – review & editing, Validation, Supervision, Resources, Project administration, Funding acquisition, Conceptualization.

Declaration of competing interest

The authors declare that they have no known competing financial interests or personal relationships that could have appeared to influence the work reported in this paper.

Acknowledgements

The authors would like to acknowledge collaborators from the University College of London (UCL): Richard Jackman, Calum Henderson, Rebecca Watkins and Jingfan Yang for fruitful discussion and exchanges. Authors gratefully acknowledge the Engineering and Physical Sciences Research Council (EPSRC), United Kingdom under grant number EP/X000176/1 for providing financial support for this research.

Data availability

Data will be made available on request.

References

[1] D. Michez, J. Letellier, I. Hammas, J. Pernot, N. Rouger, Over 50 mA current in interdigitated diamond field effect transistor, IEEE Electron Device Lett. 45 (11) (2024) 2058–2061, http://dx.doi.org/10.1109/LED.2024.3453504.

[2] P. Sittimart, Y. Sasaguri, S. Tunmee, T. Yoshitake, K. Ishiji, S. Ohmagari, Enlargement of effective area in Schottky barrier diodes on heteroepitaxial (001) diamond substrates by defect reduction and their radiation tolerance, Diam. Relat. Mater. 147 (2024) 111346, http://dx.doi.org/10.1016/j.diamond.2024.111346.

[3] X. Zhang, M. Xu, Z.K. Ng, R. Vajtai, E.H.T. Teo, Y. Zhao, P.M. Ajayan, Diamond: Recent progress in synthesis and its potential in electronics, Chem. Mater. 37 (8) (2025) 2679–2698, http://dx.doi.org/10.1021/acs.chemmater.5c00248.

[4] A. Tallaire, J. Achard, F. Silva, O. Brinza, A. Gicquel, Growth of large size diamond single crystals by plasma assisted chemical vapour deposition: Recent achievements and remaining challenges, C. R. Phys. 14 (2–3) (2013) 169–184, http://dx.doi.org/10.1016/j.crhy.2012.10.008.

[5] D. Tran, C. Mannequin, M. Bonvalot, A. Traoré, H. Mariette, M. Sasaki, E. Gheeraert, Thermal catalytic etching of diamond by double-metal layers, Diam. Relat. Mater. 145 (2024) 111075, http://dx.doi.org/10.1016/j.diamond.2024.111075.

[6] A. Maréchal, N. Rouger, J.-C. Crébier, J. Pernot, S. Koizumi, T. Teraji, E. Gheeraert, Model implementation towards the prediction of J(V) characteristics in diamond bipolar device simulations, Diam. Relat. Mater. 43 (2014) 34–42, http://dx.doi.org/10.1016/j.diamond.2014.01.009.

[7] N. Donato, M. Antoniou, E. Napoli, G. Amaratunga, F. Udrea, On the models used for TCAD simulations of Diamond Schottky Barrier Diodes, in: 2015 International Semiconductor Conference, CAS, IEEE, Sinaia, Romania, 2015, pp. 223–226, http://dx.doi.org/10.1109/SMICND.2015.7355214.

[8] H. Umezawa, Recent advances in diamond power semiconductor devices, Mater. Sci. Semicond. Process. 78 (2018) 147–156, http://dx.doi.org/10.1016/j.mssp.2018.01.007.

[9] O. Seok, M.-W. Ha, Effects of incomplete ionization on forward current–voltage characteristics of p-type diamond Schottky barrier diodes based on numerical simulation, Japan. J. Appl. Phys. 60 (SC) (2021) SCCE08, http://dx.doi.org/10.35848/1347-4065/abf2a7.

[10] S. Rashid, A. Tajani, L. Coulbeck, M. Brezeanu, A. Garraway, T. Butler, N. Rupesinghe, D. Twitchen, G. Amaratunga, F. Udrea, P. Taylor, M. Dixon, J. Isberg, Modelling of single-crystal diamond Schottky diodes for high-voltage applications, Diam. Relat. Mater. 15 (2–3) (2006) 317–323, http://dx.doi.org/10.1016/j.diamond.2005.06.019.

[11] H. Surdi, M. Bressler, M.F. Ahmad, F. Koeck, B. Winters, S. Goodnick, T. Thornton, R.J. Nemanich, J. Chang, P-i-N and Schottky P-i-N diamond diodes for high power limiters, Appl. Phys. Lett. 124 (6) (2024) 062104, http://dx.doi.org/10.1063/5.0176966.

[12] N. Donato, Modelling and Design of Diamond Power Semiconductor Devices, Apollo - University of Cambridge Repository, 2019, http://dx.doi.org/10.17863/CAM.47125.

[13] P.G. Neudeck, C. Fazi, High-field fast-risetime pulse failures in 4H- and 6H-SiC *pn* junction diodes, J. Appl. Phys. 80 (2) (1996) 1219–1225, http://dx.doi.org/10.1063/1.362922.

[14] M. Lades, W. Kaindl, N. Kaminski, E. Niemann, G. Wachutka, Dynamics of incomplete ionized dopants and their impact on 4H/6H-SiC devices, IEEE Trans. Electron Devices 46 (3) (1999) 598–604, http://dx.doi.org/10.1109/16.748884.

[15] N. Donato, F. Udrea, Static and dynamic effects of the incomplete ionization in superjunction devices, IEEE Trans. Electron Devices 65 (10) (2018) 4469–4475, http://dx.doi.org/10.1109/TED.2018.2867058.

[16] D. Li, T. Wang, W. Lin, Y. Zhu, Q. Wang, X. Lv, L. Li, G. Zou, Design of vertical diamond Schottky barrier diode with a novel beveled junction termination extension, Diam. Relat. Mater. 128 (2022) 109300, http://dx.doi.org/10.1016/j.diamond.2022.109300.

[17] A. Nawawi, K. Tseng, Rusli, G. Amaratunga, H. Umezawa, S. Shikata, Design and optimization of planar mesa termination for diamond Schottky barrier diodes, Diam. Relat. Mater. 36 (2013) 51–57, http://dx.doi.org/10.1016/j.diamond.2013.04.009.

[18] M. Brezeanu, M. Avram, S. Rashid, G. Amaratunga, T. Butler, N. Rupesinghe, F. Udrea, A. Tajani, M. Dixon, D. Twitchen, A. Garraway, D. Chamund, P. Taylor, G. Brezeanu, Termination structures for diamond schottky barrier diodes, in: 2006 IEEE International Symposium on Power Semiconductor Devices & IC's, IEEE, Naples, Italy, 2006, pp. 1–4, http://dx.doi.org/10.1109/ISPSD.2006.1666074.

[19] S. Sze, K.K. Ng, Physics of Semiconductor Devices, first ed., Wiley, 2006, http://dx.doi.org/10.1002/0470068329.

[20] G. Wachutka, Consistent treatment of carrier emission and capture kinetics in electrothermal and energy transport models, Microelectron. J. 26 (2–3) (1995) 307–315, http://dx.doi.org/10.1016/0026-2692(95)98933-I.

[21] I. Stenger, M.-A. Pinault-Thaury, T. Kociniewski, A. Lusson, E. Chikoidze, F. Jomard, Y. Dumont, J. Chevallier, J. Barjon, Impurity-to-band activation energy in phosphorus doped diamond, J. Appl. Phys. 114 (7) (2013) 073711, http://dx.doi.org/10.1063/1.4818946.

[22] S.D. Ganichev, E. Ziemann, W. Prettl, I.N. Yassievich, A.A. Istratov, E.R. Weber, Distinction between the Poole-Frenkel and tunneling models of electric-field-stimulated carrier emission from deep levels in semiconductors, Phys. Rev. B 61 (15) (2000) 10361–10365, http://dx.doi.org/10.1103/PhysRevB.61.10361.

[23] A. Schenk, A model for the field and temperature dependence of Shockley-Read-Hall lifetimes in silicon, Solid-State Electron. 35 (11) (1992) 1585–1596, http://dx.doi.org/10.1016/0038-1101(92)90184-E.

[24] K. Driche, S. Rugen, N. Kaminski, H. Umezawa, H. Okumura, E. Gheeraert, Electric field distribution using floating metal guard rings edge-termination for Schottky diodes, Diam. Relat. Mater. 82 (2018) 160–164, http://dx.doi.org/10.1016/j.diamond.2018.01.016.

[25] H. Umezawa, S.-i. Shikata, T. Funaki, Diamond Schottky barrier diode for high-temperature, high-power, and fast switching applications, Japan. J. Appl. Phys. 53 (5S1) (2014) 05FP06, http://dx.doi.org/10.7567/JJAP.53.05FP06.

[26] J.-P. Lagrange, A. Deneuville, E. Gheeraert, Activation energy in low compensated homoepitaxial boron-doped diamond films, Diam. Relat. Mater. 7 (9) (1998) 1390–1393, http://dx.doi.org/10.1016/S0925-9635(98)00225-8.

[27] J. Pernot, S. Koizumi, Electron mobility in phosphorous doped {111} homoepitaxial diamond, Appl. Phys. Lett. 93 (5) (2008) 052105, http://dx.doi.org/10.1063/1.2969066.

[28] P.-N. Volpe, J. Pernot, P. Muret, F. Omnès, High hole mobility in boron doped diamond for power device applications, Appl. Phys. Lett. 94 (9) (2009) 092102, http://dx.doi.org/10.1063/1.3086397.

[29] A. Hiraiwa, H. Kawarada, Figure of merit of diamond power devices based on accurately estimated impact ionization processes, J. Appl. Phys. 114 (3) (2013) 034506, http://dx.doi.org/10.1063/1.4816312.

[30] N. Donato, D. Pagnano, E. Napoli, G. Longobardi, F. Udrea, Design of a normally-off diamond JFET for high power integrated applications, Diam. Relat. Mater. 78 (2017) 73–82, http://dx.doi.org/10.1016/j.diamond.2017.08.003.

[31] R. Van Overstraeten, H. De Man, Measurement of the ionization rates in diffused silicon p-n junctions, Solid-State Electron. 13 (5) (1970) 583–608, http://dx.doi.org/10.1016/0038-1101(70)90139-5.

[32] A. Hiraiwa, H. Kawarada, Blocking characteristics of diamond junctions with a punch-through design, J. Appl. Phys. 117 (12) (2015) 124503, http://dx.doi.org/10.1063/1.4916240.

[33] Y. Koide, S. Koizumi, H. Kanda, M. Suzuki, H. Yoshida, N. Sakuma, T. Ono, T. Sakai, Admittance spectroscopy for phosphorus-doped n-type diamond epilayer, Appl. Phys. Lett. 86 (23) (2005) 232105, http://dx.doi.org/10.1063/1.1944896.

[34] O. Gaudin, D.K. Troupis, R.B. Jackman, C.E. Nebel, S. Koizumi, E. Gheeraert, Charge-based deep level transient spectroscopy of phosphorous-doped homoepitaxial diamond, J. Appl. Phys. 94 (9) (2003) 5832–5843, http://dx.doi.org/10.1063/1.1616635.

[35] R. Ulbricht, S.T. Van Der Post, J.P. Goss, P.R. Briddon, R. Jones, R.U.A. Khan, M. Bonn, Single substitutional nitrogen defects revealed as electron acceptor states in diamond using ultrafast spectroscopy, Phys. Rev. B 84 (16) (2011) 165202, http://dx.doi.org/10.1103/PhysRevB.84.165202.

[36] H. Shang, Y. Jiang, Optimal design of pseudo-vertical Schottky diode with n-type junction terminal extension structure, Diam. Relat. Mater. 148 (2024) 111521, http://dx.doi.org/10.1016/j.diamond.2024.111521.

[37] H. Umezawa, H. Gima, K. Driche, Y. Kato, T. Yoshitake, Y. Mokuno, E. Gheeraert, Defect and field-enhancement characterization through electron-beam-induced current analysis, Appl. Phys. Lett. 110 (18) (2017) 182103, http://dx.doi.org/10.1063/1.4982590.

[38] C. Masante, N. Rouger, J. Pernot, Recent progress in deep-depletion diamond metal–oxide–semiconductor field-effect transistors, J. Phys. D: Appl. Phys. 54 (23) (2021) 233002, http://dx.doi.org/10.1088/1361-6463/abe8fe.

[39] X. Zhang, X. Zhang, M. Li, J. Zhang, Density distribution analysis of near-interface traps in Al2O3/diamond MOS structure, Diam. Relat. Mater. 155 (2025) 112275, http://dx.doi.org/10.1016/j.diamond.2025.112275.

[40] A. Maréchal, M. Aoukar, C. Vallée, C. Rivière, D. Eon, J. Pernot, E. Gheeraert, Energy-band diagram configuration of Al2O3/oxygen-terminated p-diamond metal-oxide-semiconductor, Appl. Phys. Lett. 107 (14) (2015) 141601, http://dx.doi.org/10.1063/1.4931123.

[41] H. Arbess, K. Isoird, S. Hamady, M. Zerarka, D. Planson, Original field plate to decrease the maximum electric field peak for high-voltage diamond Schottky diode, IEEE Trans. Electron Devices 62 (9) (2015) 2945–2951, http://dx.doi.org/10.1109/TED.2015.2456073.

[42] B. Soto, J. Cañas, M. Villar, D. Araujo, J. Pernot, Transport mechanism in O-terminated diamond/ZrO2 based MOSCAPs, Diam. Relat. Mater. 121 (2022) 108745, http://dx.doi.org/10.1016/j.diamond.2021.108745.

[43] C. Masante, M. Kah, C. Hébert, N. Rouger, J. Pernot, Non-volatile photo-switch using a diamond pn junction, Adv. Electron. Mater. 8 (1) (2022) 2100542, http://dx.doi.org/10.1002/aelm.202100542.

[44] M. Kah, N. Rouger, F. Donatini, C. Masante, F.A. Koeck, R.J. Nemanich, J. Pernot, Dynamic response to electro-optical control of diamond based non-volatile photo-switch, IEEE Electron Device Lett. 45 (8) (2024) 1532–1535, http://dx.doi.org/10.1109/LED.2024.3416059.